JOURNAL OF BACTERIOLOGY, Oct. 1993, p. 6245–6253
0021-9193/93/196245-09$02.00/0

Vol. 175, No. 19

A Nucleoside Triphosphate-Regulated, 3′ Exonucleolytic Mechanism Is Involved in Turnover of Yeast Mitochondrial RNAs

JINGJUAN MIN AND HANS PETER ZASSENHAUS*

Department of Microbiology, Saint Louis University Medical School, 1402 South Grand Boulevard, Saint Louis, Missouri 63104

Received 11 February 1993/Accepted 27 July 1993

We have employed cell-free transcription reactions with mitochondria isolated from *Saccharomyces cerevisiae* to study the mechanism of RNA turnover. The specificity of RNA turnover was preserved in these preparations, as were other RNA-processing reactions, including splicing, 3′ end formation of mRNAs, and maturation of rRNAs. Turnover of nascent RNAs was found to occur exonucleolytically; endonucleolytic cleavage products were not detected during turnover of the ω intron RNA, which was studied in detail. However, these experiments still leave open the possibility that endonucleolytic cleavage products with very short half-lives are kinetic intermediates in the decay of ω RNA. Exonucleolytic turnover was regulated by nucleotide triphosphates and required their hydrolysis. A unique signature of this regulation was that any one of the eight standard ribo- or deoxyribonucleotide triphosphates supported RNA turnover. A novel hybrid selection protocol was used to determine the turnover rates of the 5′, middle, and 3′ portions of one mitochondrial transcript, the ω intron RNA. The results suggested that degradation along that transcript occurred with a 3′→5′ polarity. The similarity between features of mitochondrial RNA turnover and the properties of a nucleotide triphosphate-dependent 3′ exoribonuclease that has been purified from yeast mitochondria suggests that this single enzyme is a key activity whose regulation is involved in the specificity of mitochondrial RNA turnover.

Mitochondrial RNAs in yeast cells exhibit a broad range of stabilities. As is the case for cytoplasmic RNAs (41), mitochondrial rRNAs and tRNAs have much longer half-lives than mRNAs (36, 37). Among the mRNAs, a 10-fold range in stabilities has been inferred from studies correlating their rates of synthesis with their steady-state levels in mitochondria (36, 37). These three classes of mitochondrial transcripts are relatively stable in comparison to other classes which turn over rapidly. For example, the group I intron ω, located within the gene for the 21S rRNA (21), is cotranscribed with the large rRNA; however, the steady-state level of ω transcripts is at least 100-fold less than that of the 21S rRNA (45). Other group 1 introns are similarly turned over at a much higher rate than their flanking, cotranscribed exon sequences (6, 14). Processed intergenic sequences are likewise rapidly degraded. This class of sequences arises because most primary transcripts in yeast mitochondria are polygenic (13, 28, 49), in which genic sequences are separated by long stretches of A+U-rich spacer sequences (16). For instance, the *oli1* gene is first transcribed as part of a polygenic transcript containing it plus the downstream *serII* tRNA and *var1* genes. The intergenic regions are excised from this primary transcript during its maturation into monogenic species and are then rapidly turned over.

Unlike nucleus-encoded RNAs, synthesis, maturation, and turnover of mitochondrial RNAs all occur within the same membrane-bound compartment. Thus, whatever mechanism(s) regulates the specificity of RNA turnover, it must be able to differentiate between rapidly turning over nascent transcripts and relatively stable mature RNAs. Furthermore, it is clear that this mechanism is under genetic regulation. For example, a nuclear mutant has been characterized in which a variety of spliced group I introns accumulate to levels much higher than those in wild types (14, 43, 50). The levels of other classes of RNAs are not affected in this mutant. Other nuclear mutants specifically down regulate the stability of individual mRNAs (22, 46). In the case of mutations in CBP1, which destabilize the *cytb* mRNA (17, 19), the protein encoded by the wild-type gene apparently interacts with RNA sequences in the 5′ untranslated leader of the *cytb* mRNA (18, 35).

To understand how the specificity of RNA turnover is regulated in mitochondria, it is essential to know the mechanism by which RNAs are degraded. Little is known about this process in yeast cells, for either mitochondrial or cytoplasmic RNAs (8, 24). From studies with other eukaryotes and bacteria, it is clear that both endo- and 3′-exoribonuclease activities participate in mRNA decay (for a review, see references 2 and 40). In several instances, for either eukaryotic or bacterial mRNAs the initial or rate-limiting step in mRNA turnover appears to be endonucleolytic scission of the transcript at discrete sites or regions within the RNA which are UA rich (1, 4, 12, 26). Indeed, the relative paucity of UA dinucleotides in mRNAs has been attributed to the necessity to protect mRNAs from UpA-selective RNases (3). Once cleaved, mRNA fragments are then rapidly degraded, apparently by the action of 3′ exoribonucleases (20, 44). Although in bacteria some mRNAs decay with an overall 5′→3′ polarity (25), this directionality is apparently not due to 5′ exoribonucleolytic activity, since no such enzyme has been detected in bacteria (2). Instead, progressive 5′→3′ endonucleolytic cuts along the transcript with subsequent 3′ exonucleolytic degradation of the released 5′ terminal fragments are thought to give rise to the observed 5′→3′ polarity (9, 10).

* Corresponding author.

In other examples, however, it appears that the initial attack in the pathway of RNA decay occurs at the 3′ end of the transcript and is catalyzed by a single-strand-specific exoribonuclease. In both eukaryotes and bacteria, hairpin loops at the 3′ end of specific transcripts have been shown to stabilize the upstream portion from decay (38, 47). Mutations of the naturally occurring 3′ loop in the histone H4 mRNA not only destabilize the transcript but also eliminate cell cycle control upon its accumulation (11, 29). Although conflicting evidence on the protective role of the poly(A) tail for mRNA stability exists (for a review, see reference 40), in some cases, it appears that decay of poly(A)$^+$ mRNAs initiates exonucleolytically at their 3′ ends following partial or complete removal of the poly(A) tail (7, 42, 44).

It is important, therefore, to determine the nucleolytic components of the mechanism that degrades mitochondrial RNAs for an understanding of how the specificity of that mechanism is regulated. In this report, we provide evidence that an exoribonucleolytic process is involved in mitochondrial RNA degradation. The polarity of turnover is apparently 3′→5′, and the exoribonucleolytic activity catalyzing turnover requires nucleotide triphosphates (NTPs). The similarity between these features of mitochondrial RNA turnover and the properties of an NTP-dependent 3′ exoribonuclease which we characterized elsewhere (31) suggests that this enzyme is a key component of the mechanism regulating turnover of mitochondrial RNAs.

MATERIALS AND METHODS

In vitro transcription. Mitochondria were prepared (15) from a *nuc1-1* yeast mutant which lacks the major mitochondrial nuclease (48). In vitro transcription reactions were performed as described by Boerner et al. and Groot et al. (5, 23), with minor modifications. Isolated mitochondria (approximately 500 μg of mitochondrial protein) were suspended in 25 μl of buffer A (20 mM Tris-HCl [pH 6.7], 150 mM KCl, 10 mM K_2PO_4 [pH 6.7], 12 mM Mg_2SO_4, 20 mM creatinine phosphate, 20 μg of rifampin per ml, 6 μg of bovine serum albumin per ml, 0.6 M mannitol) plus 12 U of creatine kinase per ml, 2.5 mM ATP, 0.5 mM CTP, 0.5 mM GTP, 20 μM UTP, and 10 μCi of [α-^{32}P]UTP (Amersham). The reaction mixture was incubated at 30°C for 10 min to pulse-label the nascent mitochondrial RNAs. A chase was performed either by adding UTP to 2 mM and further incubating or by first washing the mitochondria to remove the labeled nucleotide. In the latter case, mitochondria were centrifuged at 10,000 × *g* for 10 min at 4°C and then washed three times at 4°C in 100 μl of buffer A. Each wash consisted of suspending the mitochondria in buffer and then centrifuging them as described above. The washed mitochondria were resuspended in 25 μl of buffer A plus 12 U of creatine kinase per ml and NTPs (as indicated in the figure legends) each at 1 mM, and the suspensions were further incubated at 30°C. At various times, aliquots were removed and added to 2 volumes of buffer B (20 mM Tris-HCl [pH 7.8], 20 mM EDTA, 0.3 M sodium acetate (NaOAc), 2% sodium dodecyl sulfate, 0.1% [vol/vol] 2-mercaptoethanol) to terminate the transcription reaction. RNA was prepared by two phenol extractions and precipitation of the RNA with an equal volume of isopropanol from the solution made to 3.5 M NH_4OAc. The RNA pellet was washed twice with 70% ethanol before further analysis.

RNase T_1 digestion of oligonucleotide-RNA duplexes and hybrid selection. Procedures for RNase T_1 digestion and hybrid selection have been fully described elsewhere (33). In brief, RNA was hybridized to one or more biotinylated oligonucleotides (oligos) and then subsequently digested with RNase T_1. The heteroduplex fragments were isolated by binding to streptavidin-agarose, and then the RNA was eluted from the resin by heat denaturation. Following precipitation, RNA was analyzed by acrylamide-urea gel electrophoresis. The amount of each gene-specific RNA fragment was quantified by either densitometry of autoradiograms or by excision of the fragment from the gel and scintillation counting. The oligonucleotides were synthesized so as to contain a biotin at their 5′ ends, and their sequences were as follows:

oligo 1 TATTTACAATAAATAAGTTAGCTAATTTATTAAAAGCTTG
oligo 2 AGTTTCGGATGAAATAGTATTAGGTAATTT
oligo 3 GCTTCGCTGCTTATTGTCC
oligo 4 CTATATTGTTCAGACTATATCATTATC
oligo 5 GCTGCATAGGGTCTT
oligo 6 TTAATCAAATGAGATTTTATTTTATTTTTTTTTTTATTAATTTCATTAT
oligo 7 TTATTATTATTATAATATTTATATATTTTATAATAATTATATAAT

Other procedures. Thin-layer chromatography (TLC) of labeled nucleotides in polyethyleneimine (PEI)-cellulose F plastic sheets (EM Science) was performed in 1 M formic acid–0.5 M LiCl.

RESULTS

Specificity of RNA turnover in isolated mitochondria. Previous studies have shown that isolated mitochondria synthesize nascent transcripts that are correctly processed into mature forms (5, 23). Pulse-chase experiments have indicated but have not shown directly that the specificity of RNA turnover was retained during in vitro transcription. To quantify turnover and confirm its specificity, we utilized a novel hybrid selection protocol (see Materials and Methods and reference 33) that allowed us to monitor the fate of a predetermined segment of a specific transcript during the chase. We focused on four transcripts: the 21S rRNA, its spliced intron ω, the *oli1* mRNA, and those sequences immediately 3′ to the mature *oli1* mRNA. These are referred to as *oli1* intergenic, since they are part of the primary polygenic transcript and are located between the *oli1* gene and the adjacent downstream gene, *serII* tRNA. Each pair of transcripts, 21S rRNA plus its intron and the *oli1* mRNA plus *oli1* intergenic, are cotranscribed in vivo at a high rate (37). One member of each pair, however, is stable (the 21S rRNA and *oli1* mRNA), while the other turns over rapidly (ω intron and *oli1* intergenic). Figure 1 shows the location of the specific segment within each transcript that was analyzed by using sequence specific, biotinylated oligos.

The specificity of RNA turnover in isolated mitochondria is demonstrated quantitatively by the data shown in Fig. 2. The amounts of each transcript present at the end of the pulse (odd-numbered lanes) were compared with the amounts remaining after a 15-min chase (even-numbered lanes). During the chase, 31% of the newly synthesized 21S rRNA was degraded while 91% of the cotranscribed ω intron was degraded. That the exon and intron sequences of the 21S rRNA gene were indeed cotranscribed during the pulse was shown by the following calculation. On the basis of the uridine contents of the RNase T_1 fragments and their relative intensities in the autoradiograms, we estimated the relative rates of synthesis of the 21S rRNA and ω intron during the pulse. This calculation (from an average of six experiments) showed that the exon and intron sequences were synthesized at a ratio of 1:0.7, respectively, in close agreement with the 1:1 ratio expected for cotranscribed sequences.

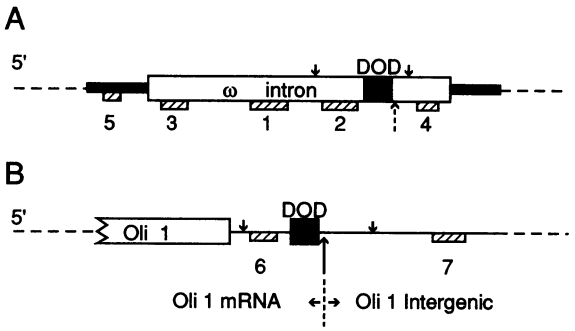

FIG. 1. Location of oligo-targeted sequences. (A) Oligos 1 to 4 were homologous to sequences within the ω intron that were located as diagrammed, whereas oligo 5 was homologous to a sequence located in the 5′ exon of the 21S rRNA. RNase T_1 digestion of oligo 2-RNA heteroduplexes (indicated by the short arrows above the diagram) generates a fragment (69 bases) which includes the 12-base dodecamer site (DOD). RNase T_1 digestion of oligo 2 heteroduplexes with RNAs that have been cleaved at the dodecamer site (indicated by the long arrow below the diagram) would generate a 57-base fragment. (B) Oligo 6 was homologous to a sequence located in the 3′ untranslated portion of the *oli1* mRNA, whereas oligo 7 annealed to a sequence located downstream of the mature mRNA 3′ end within the intergenic region between *oli1* and *serII* tRNA. RNase T_1 digestion of heteroduplexes between oligo 6 and *oli1* primary transcripts generates an approximately 230-base fragment which includes the dodecamer sequence. RNase T_1 digestion of heteroduplexes between oligo 6 and transcripts processed at the dodecamer site yields a 102-base fragment. Dashed lines indicate flanking sequences of the primary transcripts. The diagrams are not drawn to scale.

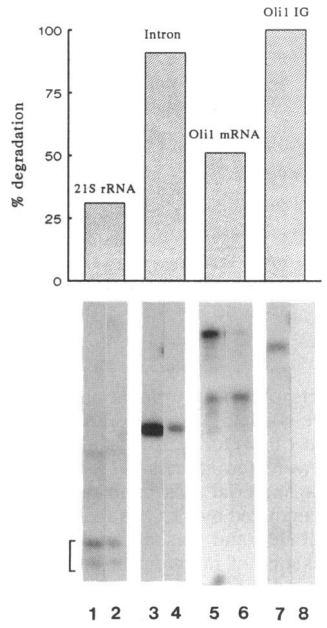

FIG. 2. Specificity of mitochondrial RNA turnover in vitro. Mitochondria were pulse-labeled with [α-^{32}P]UTP for 10 min and then chased with 100-fold excess unlabeled UTP for 15 min. RNA species (21S rRNA, ω intron, *oli1* mRNA, and *oli1* intergenic sequence [IG]) were quantified by hybrid selection of specific RNase T_1 fragments. The bar graph shows the percent degradation of each species during the chase as calculated by densitometry of the autoradiograms of a gel electrophoretic fractionation of the RNase T_1 fragments (shown below). Odd-numbered lanes, pulse-labeled RNA; even numbered lanes, pulse-chased RNA. The brackets in lanes 1 and 2 indicate cleavage fragments (25 and 23 bases) arising from RNase T_1 digestion of the 21S rRNA annealed to oligo 5. Lanes 3 and 4, ω intron-specific RNase T_1 fragment (69 bases) with oligo 2. Lanes 5 and 6, cleavage fragments arising from RNase T_1 digestion of *oli1* RNAs annealed to oligo 6. Arrows point to a larger fragment (approximately 230 bases) arising from RNase T_1 digestion of the *oli1* pre-mRNA and a smaller fragment (102 bases) resulting from RNase T_1 digestion of the mature *oli1* mRNA. Lanes 7 and 8, RNase T_1 fragment (approximately 150 bases) specific for the *oli1* intergenic sequence by using oligo 7.

The comparison of the turnover rates for the *oli1* mRNA versus the *oli1* intergenic sequences further confirmed that isolated mitochondria retained specificity for RNA degradation. During the chase, all of the *oli1* intergenic sequence was degraded (Fig. 2, lanes 7 versus 8), while only 50% of the *oli1* gene sequence was degraded (lanes 5 versus 6). The two major bands seen in lanes 5 and 6 (indicated by the arrows) derived from hybridization of the oligo probe to *oli1* pre-mRNAs (top band) versus the mature *oli1* mRNA (bottom band), as diagrammed in Fig. 1. The percent degradation of the *oli1* mRNA sequence during the chase was calculated from a comparison of the amounts of radioactivity remaining in both RNA fragments after a chase versus the amounts present after the pulse. This calculation probably overestimated the rate of degradation of the mature *oli1* mRNA. As is evident, during the chase the amount of mature mRNA increased because of maturation of pre-mRNA transcripts (cf. the intensity of the lower band in lane 5 versus lane 6).

Exonucleolytic turnover of mitochondrial RNA. To determine the nature of the enzymatic activities responsible for mitochondrial RNA turnover, we characterized the products of RNA degradation. Exoribonucleases generate mononucleotides as a degradation product, whereas endonucleases generate oligonucleotides as intermediates in RNA degradation. Oligomers between 2 and 5 nucleotides in length can readily be distinguished from either mononucleotides or larger RNAs by TLC on PEI-cellulose. Thus, characterizing the products of RNA turnover can provide information about the enzymatic activities involved in that process.

Mitochondria were pulse-labeled with [α-^{32}P]UTP for 10 min at 30°C and then washed three times at 4°C to remove unincorporated label. The mitochondria were resuspended in transcription buffer containing unlabeled NTPs, and the suspensions were further incubated at 30°C. At 0, 5, 15, and 45 min into the chase, aliquots were removed and added to a 5% solution of trichloroacetic acid (TCA). Under these conditions for RNA precipitation, oligonucleotides that were less than five nucleotides in length remain soluble whereas larger RNAs precipitate (30). A portion of the TCA supernatant was then analyzed by TLC to separate mononucleotides from small oligonucleotides.

Nearly all of the labeled TCA-soluble material comigrated with 5′ UMP (Fig. 3A). The amount of the mononucleotide increased with time coincident with the percentage of pulse-labeled RNA rendered acid soluble during the chase. When aliquots of the chase reactions were analyzed directly by TLC, without prior TCA precipitation, labeled 5′ UMP was the only detectable product that migrated away from the origin (data not shown). As is evident in Fig. 3A, the products of RNA turnover did not include detectable amounts of oligonucleotides. In this TLC system, oligonucleotides migrate with R_fs inversely proportional to their lengths; oligonucleotides up to four nucleotides in length migrate detectably away from the origin. These results

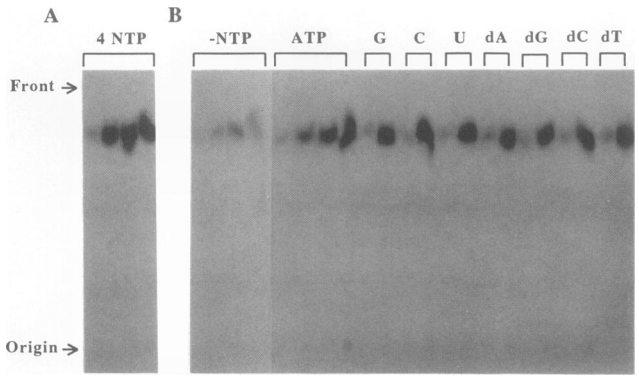

FIG. 3. Products of RNA turnover in vitro. (A) Pulse-labeled mitochondria were washed and chased in the presence of all four ribo-NTPs (each at 1 mM) for 0, 5, 15, and 45 min (lanes from left to right). Reactions were terminated by the addition of TCA to 5% (vol/vol), insoluble material was centrifuged, and aliquots of the supernatant were analyzed by TLC on PEI-cellulose. (B) Mitochondria were pulse-labeled and washed as described above and then chased in the presence of individual ribo- or deoxyribo (d)-NTPs (each at 1 mM) as indicated or in the absence of NTPs. The minus NTP and plus ATP chases were performed for 0, 5, 15, and 45 min (left to right); all others were for 0 and 45 min.

demonstrated that exonucleolytic activity was apparently responsible for the majority of RNA degradation during the chase.

NTP-stimulated exonucleolytic RNA degradation in vitro. To characterize the exonucleolytic activity(ies) responsible for RNA turnover, we investigated the dependence of RNA degradation on the presence of NTPs in the reaction mixture. Mitochondria were pulse-labeled and washed to remove free NTPs. The mitochondria were then incubated in transcription buffer containing either no NTPs or individual NTPs each at 1 mM. As shown in Fig. 3B, the generation of mononucleotide degradation products during the chase was stimulated severalfold by the presence of NTPs. Each of the individual ribo- or deoxyribonucleotides was effective in supporting RNA turnover. Note that, in the absence of NTPs during the chase, the reduced level of RNA degradation was not accompanied by the appearance of oligonucleotide digestion products. This suggests that even in the absence of NTP-dependent exonuclease activity, endonucleolytic degradation of the nascent RNAs into small oligonucleotides did not occur.

We next asked whether either nonhydrolyzable analogs of ATP (adenylyl (β,γ-methylene)-diphosphonate [AMP-PCP] and adenylyl-imidodiphosphate [AMP-PNP]) or AMP supported RNA turnover. Since nearly all of labeled TCA-soluble products were mononucleotides, we quantified RNA turnover by measuring the percentage of pulse-labeled RNA that was rendered acid soluble during the chase. Figure 4A shows that the kinetics of RNA turnover in the presence of AMP-PCP was identical to that in the absence of NTPs. In both cases, turnover was much less than when ATP was present. RNA turnover was also low in the presence of AMP or AMP-PNP, measured after a 45-min chase. Measurement of RNA turnover during a 15-min chase with respect to the concentration of ATP showed that at concentrations below 50 to 100 μM, the percent NTP-stimulated degradation decreased sharply (Fig. 4B).

Turnover of specific mitochondrial transcripts. During in vitro transcription, some nonmitochondrial RNAs were also synthesized presumably because of contamination of the mitochondrial preparation. For instance, ^{32}P-labeled killer RNA was included among the newly synthesized transcription products, as were transcripts homologous to the cytoplasmic rRNA genes. To focus more directly on the characteristics of mitochondrial RNA turnover, we used hybrid selection to examine the nucleotide requirements for turnover of the ω intron and the *oli1* intergenic sequences versus their more stable cotranscribed partners, the 21S rRNA and *oli1* mRNA.

Turnover of the ω intron versus the 21S rRNA as a function of NTPs and time is shown in Fig. 5. In this experiment, each RNA sample was incubated with a pair of biotinylated oligonucleotides; one (oligo 2) was specific for the intron, and the other (oligo 5) was specific for the 21S rRNA. RNase T_1 digestion of oligo 5-RNA heteroduplexes yielded not only the predicted fragment (Fig. 5, band 5b) but

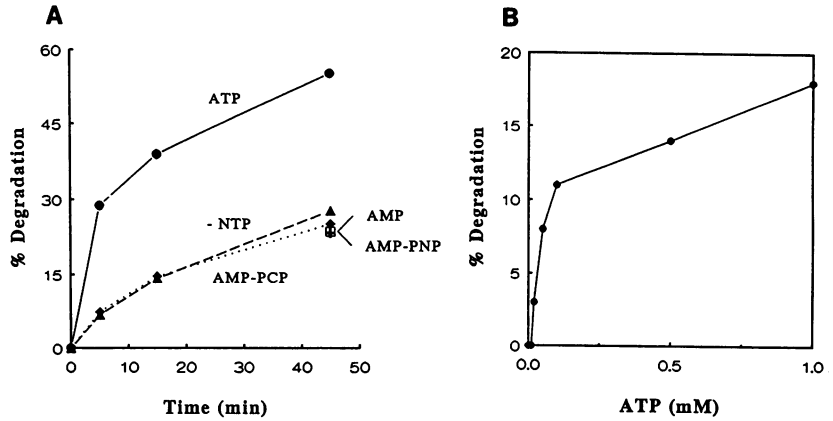

FIG. 4. Effect of nucleotides on RNA turnover in vitro. (A) Mitochondria were pulse-labeled, washed, and chased in the presence of 1 mM ATP (solid circles), AMP-PCP (solid diamonds), AMP-PNP (open square), or AMP (cross) or in the absence of NTP (solid triangles) for the indicated times. Percent degradation was calculated from the amount of material rendered TCA soluble during the chase. (B) Mitochondria were pulse-labeled, washed, and then chased in the presence of the indicated concentrations of ATP for 15 min. The ATP-stimulated percent degradation was calculated by subtraction of the amount of RNA degraded in a reaction lacking NTP from the amounts degraded in reactions containing ATP.

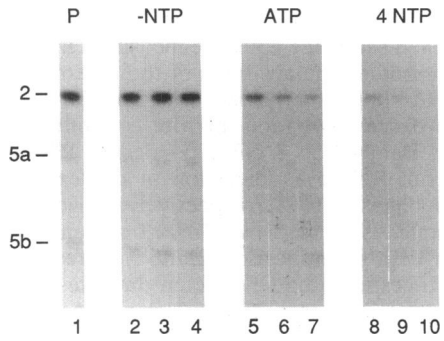

FIG. 5. Turnover of the ω intron requires NTP. Mitochondria were pulse-labeled for 10 min (P; lane 1), washed, and then chased in the absence of NTP (lanes 2 to 4) or in the presence of either 1 mM ATP (lanes 5 to 7) or 1 mM each of all four ribo-NTPs (lanes 8 to 10) for 5, 15, and 30 min (left to right in each group). RNA from each reaction was annealed to both oligo 2 (intron specific) and oligo 5 (21S rRNA specific), digested with RNase T_1, hybrid selected, and analyzed on a 15% acrylamide-urea gel.

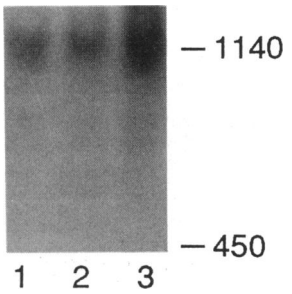

FIG. 6. Hybrid selection of ω RNAs after a chase. Mitochondria were pulse-labeled for 10 min, washed, and chased in the presence of 1 mM ATP for 15 min. Isolated RNA was separately annealed to oligos 4, 2, and 3 (lanes 1 to 3, respectively), which were homologous to segments within the intron located near its 3′ end, middle, and 5′ end, respectively. After hybrid selection and elution, the RNA was analyzed by agarose-urea gel electrophoresis (29). Sizes (in nucleotides) are indicated to the right.

also a slightly longer, partial digestion fragment (band 5a). In the absence of NTPs during the chase, little turnover was evident for the ω intron. Even after a 30-min chase (lane 4), the relative amount of the oligo 2-specific RNase T_1 fragment was nearly the same as that at the end of the pulse (lane 1; lanes 2 and 3 show the amount present after 5- and 15-min chases, respectively). However, in the presence of either ATP alone (lanes 5 to 7) or all 4 ribo-NTPs (lanes 8 to 10), rapid degradation of the intron took place during the chase. In contrast, degradation of 21S rRNA exon sequences was much slower under the same chase conditions. Densitometric analysis of these data showed that during the pulse, the molar ratio of intron to exon sequences was nearly 1:1, as expected for cotranscribed sequences. The lower autoradiographic intensity of the exon fragments was due to their sixfold lower uridine content compared with that of the intron-specific fragment. During the ATP chase, the molar ratio decreased from 0.6 (5 min) to 0.2 (30 min), and in the NTP chase it decreased from 0.4 (5 min) to <0.1 (30 min). Thus, NTP-stimulated turnover appeared to be transcript specific.

To determine whether endonucleolytic activity was also involved in the decay of the ω RNA, we asked whether large RNA fragments were detectable intermediates during ω RNA turnover (Fig. 6). These fragments were assayed by hybrid selection of ω RNAs without prior RNase T_1 digestion, followed by electrophoretic analysis of the isolated RNAs on agarose-urea gels (27). Three different biotinylated oligos were used which annealed to regions of the ω RNA located near its 3′ end (oligo 4), middle (oligo 2), and 5′ end (oligo 3; diagrammed in Fig. 1). Chase conditions in the presence of ATP as the sole NTP were employed so that turnover would be slowed down, and, consequently, so that the sensitivity for detecting kinetic intermediates would be increased. In no case did we detect the accumulation of large fragments of the spliced ω intron during its turnover (Fig. 6). In each case, the full-length spliced intron was the only detectable RNA species that was hybrid selected by the oligo. In similar experiments in which the hybrid-selected RNAs were analyzed on acrylamide gels capable of detecting fragments as small as 20 nucleotides in size, again, no fragments shorter than the full-length intron accumulated during the chase (data not shown). Although these analyses do not rule out endonucleolytic attack of the ω intron during its turnover, they do suggest that if it occurs, then the cleavage products, both 5′ and 3′ to the cleavage site(s), must decay rapidly.

The profile of nucleotides that supported turnover of ω RNA was similar to that seen for NTP stimulation of total mitochondrial RNA turnover (Fig. 4), except that ω turnover was absolutely dependent on NTPs. Neither AMP-PCP nor ADP supported turnover (Fig. 7A). Each of the individual ribo- and deoxyribo-NTPs supported turnover, but not equally well (Fig. 7B; results shown for ATP and dTTP). Least effective were deoxy-NTPs, whether individually or when all four were present; most effective was the combination of all four ribo-NTPs (Fig. 5). When combinations of three ribo-NTPs were tested, those containing ATP (e.g., ATP plus CTP plus UTP) were clearly more effective than the one lacking ATP (Fig. 7B; cf. lane -A and lane -G).

Turnover of the *oli1* intergenic sequence (Fig. 8) displayed a nucleotide dependence similar to that of turnover of the ω intron. In reaction mixtures containing either ATP or all four ribo-NTPs, the *oli1* intergenic sequence was completely degraded during the chase, whereas in reaction mixtures lacking NTPs, it was still detectable in significant amounts after a 15-min chase. In contrast, the *oli1* mRNA (lower band marked by the arrow in Fig. 8) was relatively stable during the chase regardless of the presence or absence of NTPs. It was also apparent that processing of *oli1* pre-mRNAs (Fig. 8, upper band) was stimulated by either ATP or the combina-

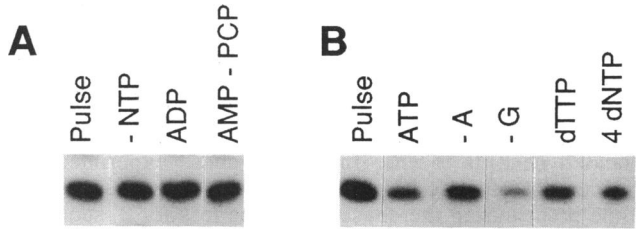

FIG. 7. Effect of different nucleotides on turnover of the ω intron. Conditions were as described in the legend to Fig. 5 with oligo 2 to probe ω RNA turnover after a 15-min chase. Nucleotides (when indicated) were present at 1 mM each. −A, CTP plus UTP plus GTP; −G, ATP plus CTP plus UTP; 4 dNTP, dATP plus dCTP plus dTTP plus dGTP.

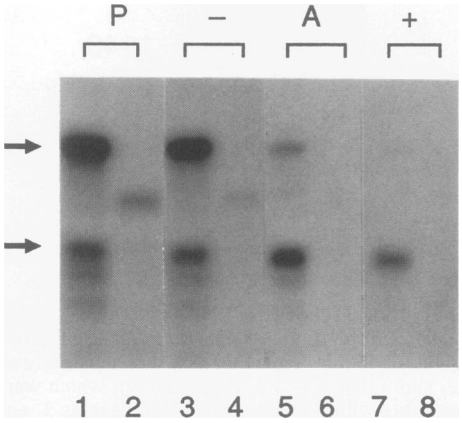

FIG. 8. Effect of NTP on turnover and processing of *oli1* transcripts. Mitochondria were pulse-labeled (P; lanes 1 and 2), washed, and then chased for 15 min in the absence of NTPs (lanes 3 and 4) or in the presence of either 1 mM ATP (A; lanes 5 and 6) or 1 mM each of all four ribo-NTPs (lanes 7 and 8). Each RNA sample was annealed either to oligo 6 (specific for *oli1* mRNA sequences; odd-numbered lanes) or to oligo 7 (specific for *oli1* intergenic sequences; even-numbered lanes). The annealed samples were then digested with RNase T_1, hybrid selected, and analyzed on a 15% acrylamide-urea gel. The arrows indicate cleavage fragments resulting from oligo 6 annealed to either the pre-mRNA (upper band) or to the processed, mature mRNA (lower band), as diagrammed in Fig. 1.

tion of all four ribo-NTPs. The 3′ end of the mature *oli1* mRNA, like all other mitochondrial mRNAs, is formed by a site-specific endonucleolytic cleavage of pre-mRNAs at a conserved 12-nucleotide sequence termed the dodecamer site (14, 39). The lower band in Fig. 8 arose from precise cleavage of pre-mRNAs at the *oli1* dodecamer site (Fig. 1), as determined by the comigration on sequencing gels of this hybrid-selected, labeled RNase T_1 fragment with a similarly prepared fragment using isolated, in vivo-synthesized mitochondrial RNA (data not shown). During the 10-min pulse-labeling, a significant fraction of newly made *oli1* transcripts was cleaved at the dodecamer site, a fraction which did not increase during a chase in the absence of NTPs. However, in the presence of ATP, the amount of dodecamer-cleaved RNA increased during the chase while the amount of uncleaved pre-mRNA decreased, suggesting a precursor-product relationship. With all four NTPs present, this relationship was not as evident in this experiment, although it was more evident in other similar experiments (e.g., Fig. 2).

Polarity of mitochondrial RNA degradation. Since turnover of the ω RNA appeared to occur by an NTP-dependent exonucleolytic process, we focused on that transcript to investigate the directionality of mitochondrial RNA turnover. We reasoned that if degradation occurred 3′ to 5′ through the ω RNA, then among a population of partially degraded molecules the relative abundance of a sequence located near its 3′ end should be less than that of a sequence located near its 5′ end. In a pulse-chase experiment, the percentage of pulse-labeled material remaining at any given time point during the chase should be less for 3′ sequences than for 5′ sequences. To measure the relative abundance of different regions of the ω RNA, we employed a set of four biotinylated oligonucleotides that were homologous to sequences of the ω intron located near it 5′ end, middle, and 3′ end (diagrammed in Fig. 1). Each sequence was chosen so that RNase T_1 digestion of the RNA-oligonucleotide duplex generated a fragment with a unique size. Thus, the abundance of each sequence could be measured in a single RNA sample, improving the accuracy of the determinations.

Figure 9A shows the gel patterns from an experiment in which the chase incubation mixture contained ATP as the sole NTP. Bands 1 to 4 corresponded to RNA fragments derived from RNase T_1 digestion of duplexes between ω RNA and oligos 1 to 4, respectively. Digestion of oligo 1-RNA duplexes yielded two RNA fragments which were pooled for their quantification. Band 5 corresponded to the RNase T_1 digestion product of heteroduplexes between oligo 5 and exon sequences of the 21S rRNA (Fig. 1). The percentage of pulse-labeled ω RNA that remained as a function of its location within the intron is plotted in the accompanying graph in Fig. 9B. A distinct 3′→5′ polarity in the turnover of the ω intron was observed, as manifested by the rising slope of the curves which showed that sequences near the 3′ end of the intron turned over more rapidly than those near its 5′ end. Interestingly, however, the greatest amount of degradation was observed not for the most 3′-terminal sequence, but rather for the oligo 2-specific sequence located 155 bases from the 3′ end (Fig. 1).

Pooling results from a number of experiments showed that the apparent 3′→5′ polarity in ω RNA degradation, as well as the rapid decay of sequences adjacent to oligo 2, was consistently observed (Fig. 9C). In these experiments, the absolute level of turnover differed because of various NTPs present during the chase and various durations of chase between 5 and 30 min. To pool results, the differences in the abundance between a given sequence and the oligo 2-specific sequence located 155 bases from the 3′ end were calculated in each experiment. These differences were averaged and plotted as shown in Fig. 9C. One interpretation for the dip in the polarity curve is that some fraction of ω RNAs is degraded not only from their 3′ terminus but also in a 3′→5′ direction initiating at an endonucleolytic scission made at a site adjacent to the sequence probed for by oligo 2.

Immediately 3′ to the oligo 2-specific sequence in ω is situated a dodecamer site which is located about 130 bases from the 3′ end of the intron (Fig. 1). From mapping studies, it is known that a proportion of nascent ω transcripts is cleaved at that site in vivo (39); whether they were likewise cleaved under our in vitro conditions is not clear. Cleavage at a similar dodecamer site in *oli1* transcripts occurred in the isolated mitochondria as presented above (Fig. 2 and 8); however, the characteristic RNase T_1 fragment from oligo 2 heteroduplexes (Fig. 1), which would indicate cleavage at the dodecamer site in ω RNA, was not observed (Fig. 2, 5, and 9). Neither did we detect during ω RNA turnover the accumulation of the approximately 130-base downstream fragment that would be predicted to arise from cleavage of ω RNAs at its dodecamer site (data not shown). Thus, if some fraction of ω RNAs initiated turnover from a cut made at the dodecamer site, then the cleavage products apparently were short-lived.

DISCUSSION

The data presented here show that turnover of nascent RNAs in mitochondria requires NTP, employs exoribonuclease activity, and appears to proceed in a 3′-to-5′ direction along at least one transcript, the ω intron RNA. The evidence for these conclusions comes from studies on the fate of newly made RNAs in isolated mitochondria during in vitro transcription reactions. Several features of the cell-free transcription system argue that the properties of RNA turn-

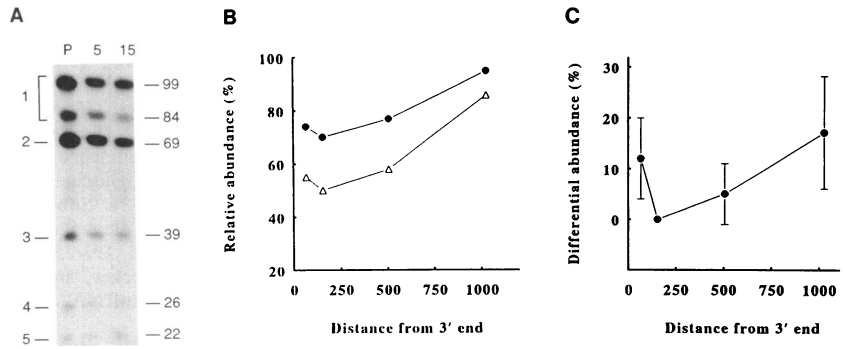

FIG. 9. Polarity of ω RNA turnover. (A) Mitochondria were pulse-labeled (P), washed, and chased in the presence of 1 mM ATP for 5 and 15 min. Each RNA sample was annealed to a mixture of oligos, of which four (oligos 1 to 4) were homologous to the ω intron, while the fifth, oligo 5, annealed to a 21S rRNA exon sequence (Fig. 1). Following RNase T_1 digestion and hybrid selection, the cleavage fragments were fractionated on a 15% acrylamide-urea gel. On the left are indicated the RNase T_1 fragments specific to each numbered oligo; the sizes (in nucleotides) of the fragments are indicated on the right. (B) The radioactivities in bands 1 to 4 from the gel shown in panel A were determined by scintillation counting. From these determinations, the relative abundance of each sequence in the chase sample, as a percentage of the amount present immediately after the pulse, was plotted as a function of the distance of the sequence from the 3′ end of the spliced intron. (C) Results from 18 separate determinations similar to the ones shown in panels A and B were pooled as described in the text. The relative abundance after a chase of the oligo 2-specific sequence was used as the reference, which was subtracted from the values for the other sequences in each experiment. The average differences ± standard errors of the mean are plotted. Quantification was either by scintillation counting of excised gel fragments or by densitometry of gel autoradiograms.

over determined in vitro accurately reflect the mechanism of turnover in vivo. First, the specificity of turnover was maintained in vitro; mature mRNAs and rRNAs were stable, while intergenic sequences and the group 1 ω intron rapidly turned over. Second, several different RNA-processing reactions still functioned normally, as evidenced by splicing of the ω intron and precise 3′ end formation of the *oli1* mRNA by cleavage at the dodecamer site in its precursor. In agreement with previous observations (5, 23), mature 14S and 21S rRNAs were also synthesized, as judged by their comigration on gels with authentic counterparts (data not shown). Both of these transcripts require precise endonucleolytic processing for their maturation.

That an exoribonucleolytic mechanism is involved in RNA turnover was demonstrated by two observations: (i) the vast majority of degradation products were exclusively 5′ nucleotide monophosphates, and (ii) endonucleolytically derived RNA fragments, either large or small, were not detected as kinetic intermediates in RNA turnover. Generally, exonucleases degrade RNA processively to yield nucleotide monophosphates as the immediate digestion product (2). In contrast, endonucleases are distributive enzymes that degrade RNA to progressively smaller fragments before yielding oligonucleotides and nucleotide monophosphates as the final digestion product. Thus, exoribonucleolytic activity appears to account for most of the degradation into mononucleotides of nascent RNAs within mitochondria.

Exoribonucleolytic degradation of mitochondrial RNA was stimulated by, and possibly dependent on, NTPs. A unique signature of mitochondrial RNA decay was that any one of the eight standard ribo- and deoxyribo-NTPs supported RNA turnover. Hydrolysis of the β-γ phosphodiester bond in a triphosphate was apparently necessary for RNA degradation, since neither nonhydrolyzable analogs of ATP (AMP-PCP and AMP-PNP) nor nucleotide mono- or diphosphates supported RNA degradation.

The nucleotide requirement for RNA turnover in isolated mitochondria correlates with the cofactor requirements of a 3′ exoribonuclease that we have isolated from yeast mitochondria (31, 32). Like RNA turnover, a unique signature of this enzyme is that its activity in vitro is dependent on NTPs and that each of the eight ribo- or deoxyribo-NTPs supports activity equally well. Like RNA turnover, neither nonhydrolyzable analogs of ATP nor AMP and ADP support activity of the 3′ exoribonuclease. Moreover, the K_m of the enzyme for ATP (40 μM) is in the same range of ATP concentration (50 to 100 μM) which supported RNA turnover in the isolated organelle. Since the isolated 3′ exoribonuclease is the only detectable exoribonucleolytic activity in these mitochondria (31), it would appear that RNA turnover is catalyzed predominantly by this enzyme.

Whether the activity of that NTP-dependent 3′ exoribonuclease is the key regulatory step in mitochondrial RNA turnover, however, depends in part on the pathway of RNA degradation. If RNAs are first cleaved endonucleolytically before final degradation into mononucleotides by that enzyme, then it would be unlikely that its regulation determines the specific half-lives of the various RNAs found within mitochondria. To gain insight into the pathway of RNA decay, we investigated the polarity of degradation of the ω RNA. By determining the relative abundance of four different regions of the ω intron at various times after its synthesis, we found that sequences near its 3′ end turn over faster than sequences near its 5′ end. Furthermore, neither large nor small cleavage fragments were detected as kinetic intermediates during degradation of ω RNA. These data are consistent with a mechanism of RNA decay that initiates at the 3′ end of an RNA molecule, proceeds 3′→5′ along it, and is catalyzed by the NTP-dependent 3′ exoribonuclease. The absence of detectable degradation of ω RNA in the absence of NTPs also supports the key role of the exoribonuclease in this model. However, at least two caveats to this interpretation must be noted.

First, the apparent 3′→5′ polarity of ω RNA degradation may be due to a systematic error in the hybrid selection protocol that leads to differential detection of intron sequences located in the 5′, middle, and 3′ regions of the RNA. We think that this explanation is unlikely, since with pulse-labeled RNA the molar amounts were all approximately equal for the segments probed for by the four oligos em-

ployed in these experiments. Only during a chase in the presence of NTPs did the stoichiometry significantly change so that 3′ sequences became less abundant than 5′ sequences.

Second, these experiments do not rule out the possibility that an endonuclease(s) initiates RNA decay which is followed by rapid 3′ exonucleolytic degradation of the cleavage products. Such a mechanism would explain the absence of detectable RNA fragments as kinetic intermediates during ω RNA decay. Moreover, the apparent directionality of ω RNA decay might than reflect the differential susceptibilities of the various intron RNA segments to endonucleolytic attack. The dodecamer site within ω RNA, for example, could be a preferential cleavage site, explaining the observation that sequences 5′ to that site were the most rapidly decaying among those that we studied. If so, then in yeast mitochondria, endonucleolytic attack on an RNA appears also to be dependent on NTPs, since in their absence little ω RNA degradation, whether endo- or exonucleolytic, was observed.

Whether RNA decay initiates endo- or exonucleolytically from the 3′ end, a mechanism would seem to be required to protect stable mitochondrial RNAs from attack by the NTP-dependent 3′ exoribonuclease. In prokaryotes, hairpin loops at the 3′ ends of some mRNAs have been shown to be necessary for their stability (26, 38). In yeast mitochondria, inspection of the nucleotide sequence at the 3′ ends of mRNAs does not reveal the presence of stable stem-loop structures. We have recently shown that mitochondria contain a protein complex which specifically binds to the 3′ ends of mitochondrial mRNAs (34). In vitro, RNAs bound to that complex are resistant to digestion by the NTP-dependent 3′ exoribonuclease. This complex and the 3′ exoribonuclease, along with other factors, are likely candidates for components of the mechanism that regulates RNA stability in yeast mitochondria.

ACKNOWLEDGMENTS

This work was supported by a grant (DCB-9018612) from the National Science Foundation.

We thank Tana McKerrow for her excellent word-processing assistance.

REFERENCES

1. **Babitzke, P., and S. R. Kushner.** 1991. The Ams (altered mRNA stability) protein and ribonuclease E are encoded by the same structural gene of Escherichia coli. Proc. Natl. Acad. Sci. USA **88**:1–5.
2. **Belasco, J. G., and C. F. Higgins.** 1988. Mechanisms of mRNA decay in bacteria: a perspective. Gene **72**:15–23.
3. **Beutler, E., T. Gelbart, J. H. Han, J. A. Koziol, and B. Beutler.** 1989. Evolution of the genome and the genetic code: selection at the dinucleotide level by methylation and polyribonucleotide cleavage. Proc. Natl. Acad. Sci. USA **86**:192–196.
4. **Binder, R., S. P. Hwang, R. Ratnasabapathy, and D. L. Williams.** 1989. Degradation of apolipoprotein II mRNA occurs via endonucleolytic cleavage at 5′-AAU-3′/5′-UAA-3′ elements in single-stranded loop domains of the 3′-noncoding region. J. Biol. Chem. **264**:16910–16918.
5. **Boerner, P., T. L. Mason, and T. D. Fox.** 1981. Synthesis and processing of ribosomal RNA in isolated yeast mitochondria. Nucleic Acids Res. **9**:6379–6390.
6. **Bonitz, S. G., G. Homison, B. E. Thalenfeld, A. Tzagoloff, and F. G. Nobrega.** 1982. Assembly of the mitochondrial membrane system. Processing of the apocytochrome b precursor RNAs in Saccharomyces cerevisiae D273-10B. J. Biol. Chem. **257**:6268–6274.
7. **Brewer, G., and J. Ross.** 1988. Poly(A) shortening and degradation of the 3′ A+U-rich sequences of human c-*myc* mRNA in a cell-free system. Mol. Cell. Biol. **8**:1697–1708.
8. **Brown, A. J., I. J. Purvis, T. C. Santiago, A. J. Bettany, L. Loughlin, and J. Moore.** 1988. Messenger RNA degradation in Saccharomyces cerevisiae. Gene **72**:151–160.
9. **Cannistraro, V. J., and D. Kennell.** 1989. Purification and characterization of ribonuclease M and mRNA degradation in Escherichia coli. Eur. J. Biochem. **181**:363–370.
10. **Cannistraro, V. J., M. N. Subbarao, and D. Kennell.** 1986. Specific endonucleolytic cleavage sites for decay of Escherichia coli mRNA. J. Mol. Biol. **192**:257–274.
11. **Capasso, O., G. C. Bleecker, and N. Heintz.** 1987. Sequences controlling histone H4 mRNA abundance. EMBO J. **6**:1825–1831.
12. **Chen, C. Y., and J. G. Belasco.** 1990. Degradation of pufLMX mRNA in *Rhodobacter capsulatus* is initiated by nonrandom endonucleolytic cleavage. J. Bacteriol. **172**:4578–4586.
13. **Christianson, T., J. C. Edwards, D. M. Mueller, and M. Rabinowitz.** 1983. Identification of a single transcriptional initiation site for the glutamic tRNA and COB genes in yeast mitochondria. Proc. Natl. Acad. Sci. USA **80**:5564–5568.
14. **Conrad-Webb, H., P. S. Perlman, H. Zhu, and R. A. Butow.** 1990. The nuclear SUV3-1 mutation affects a variety of post-transcriptional processes in yeast mitochondria. Nucleic Acids Res. **18**:1369–1376.
15. **Dake, E., T. J. Hofmann, S. McIntire, A. Hudson, and H. P. Zassenhaus.** 1988. Purification and properties of the major nuclease from mitochondria of Saccharomyces cerevisiae. J. Biol. Chem. **263**:7691–7702.
16. **de Zamaroczy, M., and G. Bernardi.** 1987. The AT spacers and the var1 genes from the mitochondrial genomes of Saccharomyces cerevisiae and Torulopsis glabrata: evolutionary origin and mechanism of formation. Gene **54**:1–22.
17. **Dieckmann, C. L., T. J. Koerner, and A. Tzagoloff.** 1984. Assembly of the mitochondrial membrane system. CBP1, a yeast nuclear gene involved in 5′ end processing of cytochrome b pre-mRNA. J. Biol. Chem. **259**:4722–4731.
18. **Dieckmann, C. L., and T. M. Mittelmeier.** 1987. Nuclearly-encoded CBP1 interacts with the 5′ end of mitochondrial cytochrome b pre-mRNA. Curr. Genet. **12**:391–397.
19. **Dieckmann, C. L., L. K. Pape, and A. Tzagoloff.** 1982. Identification and cloning of a yeast nuclear gene (CBP1) involved in expression of mitochondrial cytochrome b. Proc. Natl. Acad. Sci. USA **79**:1805–1809.
20. **Donovan, W. P., and S. R. Kushner.** 1986. Polynucleotide phosphorylase and ribonuclease II are required for cell viability and mRNA turnover in Escherichia coli K-12. Proc. Natl. Acad. Sci. USA **83**:120–124.
21. **Dujon, B.** 1980. Sequence of the intron and flanking exons of the mitochondrial 21S rRNA gene of yeast strains having different alleles at the omega and rib-1 loci. Cell **20**:185–197.
22. **Grivell, L. A.** 1989. Nucleo-mitochondrial interactions in yeast mitochondrial biogenesis. Eur. J. Biochem. **182**:477–493.
23. **Groot, G. S., N. van Harten-Loosbroek, G. J. Van Ommen, and H. L. Pijst.** 1981. RNA synthesis in isolated yeast mitochondria. Nucleic Acids Res. **9**:6369–6377.
24. **Herrick, D., R. Parker, and A. Jacobson.** 1990. Identification and comparison of stable and unstable mRNAs in *Saccharomyces cerevisiae*. Mol. Cell. Biol. **10**:2269–2284.
25. **Kennell, D. E.** 1987. The instability of messenger RNA in bacteria, p. 101–143. *In* W. Reznikoff and L. Gold (ed.), Maximizing gene expression. Butterworths Publishers, London.
26. **Klug, G., and S. N. Cohen.** 1990. Combined actions of multiple hairpin loop structures and sites of rate-limiting endonucleolytic cleavage determine differential degradation rates of individual segments within polycistronic *puf* operon mRNA. J. Bacteriol. **172**:5140–5146.
27. **Locker, J.** 1979. Analytical and preparative electrophoresis of RNA in agarose-urea. Anal. Biochem. **98**:358–367.
28. **Locker, J., and M. Rabinowitz.** 1981. Transcription in yeast mitochondria: analysis of the 21 S rRNA region and its transcripts. Plasmid **6**:302–314.
29. **Luscher, B., C. Stauber, R. Schindler, and D. Schumperli.** 1985.

Faithful cell-cycle regulation of a recombinant mouse histone H4 gene is controlled by sequences in the 3'-terminal part of the gene. Proc. Natl. Acad. Sci. USA **82**:4389–4393.

30. **Maniatis, T., E. F. Fritsch, and J. Sambrook.** 1982. Molecular cloning: a laboratory manual. Cold Spring Harbor Laboratory, Cold Spring Harbor, N.Y.
31. **Min, J., R. M. Heuertz, and H. P. Zassenhaus.** 1993. Isolation and characterization of an NTP-dependent 3'-exoribonuclease from mitochondria of *Saccharomyces cerevisiae*. J. Biol. Chem. **268**:7350–7357.
32. **Min, J., and H. P. Zassenhaus.** 1991. Characterization of a novel NTP-dependent 3' exoribonuclease from yeast mitochondria. SAAS Bull. Biochem. Biotech. **4**:1–5.
33. **Min, J., and H. P. Zassenhaus.** 1992. Quantitation of radioactively labeled RNA by hybrid selection using biotinylated oligonucleotides. BioTechniques **13**:870–874.
34. **Min, J., and H. P. Zassenhaus.** 1993. Identification of a protein complex that binds to a dodecamer sequence found at the 3' ends of yeast mitochondrial mRNAs. Mol. Cell. Biol. **13**:4167–4173.
35. **Mittelmeier, T. M., and C. L. Dieckmann.** 1990. CBP1 function is required for stability of a hybrid cob-oli1 transcript in yeast mitochondria. Curr. Genet. **18**:421–428.
36. **Mueller, D. M., and G. S. Getz.** 1986. Steady state analysis of mitochondrial RNA after growth of yeast Saccharomyces cerevisiae under catabolite repression and derepression. J. Biol. Chem. **261**:11816–11822.
37. **Mueller, D. M., and G. S. Getz.** 1986. Transcriptional regulation of the mitochondrial genome of yeast Saccharomyces cerevisiae. J. Biol. Chem. **261**:11756–11764.
38. **Newbury, S. F., N. H. Smith, E. C. Robinson, I. D. Hiles, and C. F. Higgins.** 1987. Stabilization of translationally active mRNA by prokaryotic REP sequences. Cell **48**:297–310.
39. **Osinga, K. A., E. De Vries, G. Van der Horst, and H. F. Tabak.** 1984. Processing of yeast mitochondrial messenger RNAs at a conserved dodecamer sequence. EMBO J. **3**:829–834.
40. **Peltz, S. W., G. Brewer, P. Bernstein, P. A. Hart, and J. Ross.** 1991. Regulation of mRNA turnover in eukaryotic cells. Crit. Rev. Eukaryotic Gene Expression **1**:99–126.
41. **Santiago, T. C., I. J. Purvis, A. J. Bettany, and A. J. Brown.** 1986. The relationship between mRNA stability and length in Saccharomyces cerevisiae. Nucleic Acids Res. **14**:8347–8360.
42. **Shyu, A. B., J. G. Belasco, and M. E. Greenberg.** 1991. Two distinct destabilizing elements in the c-fos message trigger deadenylation as a first step in rapid mRNA decay. Genes Dev. **5**:221–231.
43. **Stepien, P. P., S. P. Margossian, D. Landsman, and R. A. Butow.** 1992. The yeast nuclear gene suv3 affecting mitochondrial post-transcriptional processes encodes a putative ATP-dependent RNA helicase. Proc. Natl. Acad. Sci. USA **89**:6813–6817.
44. **Swartwout, S. G., and A. J. Kinniburgh.** 1989. c-*myc* RNA degradation in growing and differentiating cells: possible alternate pathways. Mol. Cell. Biol. **9**:288–295.
45. **Tabak, H. F., G. Van der Horst, K. A. Osinga, and A. C. Arnberg.** 1984. Splicing of large ribosomal precursor RNA and processing of intron RNA in yeast mitochondria. Cell **39**:623–629.
46. **Tzagoloff, A., and A. M. Myers.** 1986. Genetics of mitochondrial biogenesis. Annu. Rev. Biochem. **55**:249–285.
47. **Xing, Y. Y., and A. Worcel.** 1989. A 3' exonuclease activity degrades the pseudogene 5S RNA transcript and processes the major oocyte 5S RNA transcript in Xenopus oocytes. Genes Dev. **3**:1008–1018.
48. **Zassenhaus, H. P., T. J. Hofmann, R. Uthayashanker, R. D. Vincent, and M. Zona.** 1988. Construction of a yeast mutant lacking the mitochondrial nuclease. Nucleic Acids Res. **16**: 3283–3296.
49. **Zassenhaus, H. P., N. C. Martin, and R. A. Butow.** 1984. Origins of transcripts of the yeast mitochondrial var 1 gene. J. Biol. Chem. **259**:6019–6027.
50. **Zhu, H., H. Conrad-Webb, X. S. Liao, P. S. Perlman, and R. A. Butow.** 1989. Functional expression of a yeast mitochondrial intron-encoded protein requires RNA processing at a conserved dodecamer sequence at the 3' end of the gene. Mol. Cell. Biol. **9**:1507–1512.